

**Discrete-time design of tracking control loop
for optical communications**

**Homayoon Ansari
Jet Propulsion Laboratory
4800 Oak Grove Drive
Pasadena, CA 91109**

Abstract

The methodology for discrete-time design of a fine steering mirror tracking control loop is presented. It is shown that high tracking accuracy can be achieved for optical communications by using low cost fine steering mirrors and moderate sampling rates.

Key words optical communications, tracking, discrete-time control systems.

Optical communication requires accurate and stable pointing of a transmit laser beam in the presence of platform jitter in order to achieve and maintain high data rates. High bandwidth fine steering mirrors are typically used to stabilize the receive line of sight (LOS) in optical communication systems, allowing a second low bandwidth steering mechanism to point ahead the transmit laser beam towards the receiver. Recently, a new technique has been proposed [1] which uses only a single fine steering mirror and a single fast CCD array detector for precision beam pointing. In this technique, the receive LOS is not stabilized but the transmit laser beam tracks the receive beam on the CCD array with proper point-ahead and with high accuracy.

The purpose of the tracking control loop in optical communications is to achieve stable and accurate beam pointing in the presence of platform jitter. Digital implementation of control loops allows greater design flexibility and reduced controller parameter variations compared to analog control loops. However, the performance of digital control loops is limited by the sampling rate. Any delay in reading out the sensor and digital processing can also limit the control loop performance. In addition, in either digital or analog tracking control loops, the frequency response characteristics of the fine steering mirror can limit the performance.

This paper shows that high pointing accuracy can be achieved for optical communications, given the Landsat-type platform jitter spectrum [2,3], by using a digital tracking control loop that incorporates 1) a low cost commercial fine steering mirror with a low primary resonance frequency of 17 Hz, 2) a moderate sampling rate of 2 KHz, and 3) a pure delay of one sampling period or 0.5 msec. The design and analysis are all carried out directly in the z-plane such that the performance of the system can be accurately predicted at high frequencies and optimized.

Figure 1 shows the basic block diagram of the control loop. In figure 1, $H_m(z)$ is the cascaded transfer function of Zero Order Hold (ZOH), fine steering mirror, sensor electronics, and the pure delay, and $H_c(z)$ is the transfer function of control loop compensation. The reference input can be the desired point-ahead and the output is then the actual point-ahead.

From classical control theory [4], the discrete-time transfer function of a continuous-time plant preceded by ZOH is,

$$H_m(z) = (1 - z^{-1}) \mathcal{Z} \left\{ \frac{H_m(s)}{s} \right\} \quad (1)$$

where $H_m(z)$ and $H_m(s)$ are the discrete-time and continuous-time transfer functions, respectively, and $\mathcal{Z}\{ \}$ denotes the z-transform of the time samples of the inverse Laplace transform of its argument. For a second-order continuous-time plant corresponding to a fine steering mirror, and after adding an arbitrary pure delay of up to one sampling period to eq.(1), we obtain,

$$H_m(z) = A_m \frac{z - z_1}{z} \frac{z - z_2}{(z - p_m)(z - p_m^*)} \quad (2)$$

where A_m is a constant, the first fraction on the RHS contains a zero and a pole that are due to the pure delay, and the second fraction on the RHS contains a zero due to ZOH and a pair of conjugate poles due to mirror resonance.

The closed loop transfer function of the control loop in figure 1 is given by,

$$H_{cl}(z) = \frac{H_c(z)H_m(z)}{1 + H_c(z)H_m(z)} \quad (3)$$

where $H_c(z)$ is the compensation transfer function. In the design, the two conjugate poles of $H_m(z)$ can be directly cancelled by placing two conjugate zeros in $H_c(z)$, which will result in enhancing the closed loop characteristics.

Direct cancellation of any pole or zero of $H_m(z)$ by $H_c(z)$ in eq.(3) would result in that pole or zero to remain in the closed loop characteristic polynomial. In the case of any

troublesome poles or zeros of $H_m(z)$, i.e. those close to or outside the unit circle in the z-plane, this method cannot be used because it will lead to instability. Instead, following the direct digital design method of Ragazzini [4], eq.(3) will be rewritten as,

$$H_c(z) = \frac{1}{H_m(z)} \frac{H_{cl}(z)}{1 - H_{cl}(z)} \quad (4)$$

Any troublesome pole or zero of $H_m(z)$ can now be cancelled by the numerator of $1 - H_{cl}(z)$ or numerator of $H_{cl}(z)$ in eq.(4), respectively.

The design of compensation $H_c(z)$ can now be completed by specifying the desired poles of $H_{cl}(z)$ in eq.(4). To satisfy causality, $H_{cl}(z)$ must have the same number of zeros at infinity as $H_m(z)$ does. For a type I control system, the desired closed loop transfer function is,

$$H_{cl}(z) = A_{cl} \frac{z - z_2}{(z - p_{cl})(z - p_{cl}^*)} \quad (5)$$

where A_{cl} is a constant, z_2 is from eq.(2), and p_{cl} and p_{cl}^* are the desired closed loop poles.

Inserting eq.(5) in eq.(4),

$$H_c(z) = A_c \frac{z}{z - z_1} \frac{(z - p_m)(z - p_m^*)}{(z - 1)(z - p_c)} \quad (6)$$

where,

$$A_c = \frac{A_{cl}}{A_m} \quad (7)$$

and

$$p_c = |p_{cl}|^2 + (1 - p_{cl})(1 - p_{cl}^*) \frac{z_2}{1 - z_2} \quad (8)$$

The transfer function of disturbance rejection is given by,

$$H_{dr}(z) = \frac{1}{1 + H_c(z)H_m(z)} \quad (9)$$

Inserting eq.(6) in eq.(9), we obtain,

$$H_{dr}(z) = \frac{(z-1)(z-p_c)}{(z-p_{cl})(z-p_{cl}^*)} \quad (10)$$

The same methodology can be extended to type 0, type II, or higher order systems. Furthermore, for pure delays of more than one sampling period, $H_m(z)$ in eq.(2) will include one extra pole at $z=0$ and one extra zero for each sampling period unit of delay.

A type I compensation was designed based on the above analysis for a tracking control loop that incorporated a fine steering mirror with a resonance frequency of 17 Hz, a sampling rate of 2 KHz, and a pure delay of 0.5 msec. The compensation provides significant phase lead at around the mirror resonance and higher frequencies to greatly improve stability, accuracy, and bandwidth of the control loop. The compensation was implemented using a TMS320C30-based Digital Signal Processing (DSP) board. A 2x2 APD detector/amplifier was used as the sensor, and a simple centroiding algorithm on the detector/amplifier output was implemented in the DSP board to obtain the error signal.

A set of measurements described below were performed on the tracking control loop to determine its performance. Figure 2 shows the frequency response of the fine steering mirror which corresponds to a second order continuous-time plant with a primary resonance frequency of 17 Hz and a damping ratio of 0.5. No secondary resonance frequencies were observed up to

1 KHz. Figure 3 shows the open-loop frequency response of the control loop that includes compensation, and can be used to obtain phase and gain margins and cross-over frequencies. Figure 4 shows the disturbance rejection of the control loop. When applying the jitter spectrum [2,3] based on Landsat and OLYMPUS studies, the disturbance rejection will result in an rms residual tracking accuracy of $2.0 \mu\text{rad}$. The measured phase and gain margins are 28 degrees and 3 dB, respectively, and the phase and gain cross-over frequencies are 290 Hz and 206 Hz, respectively. Measurement plots of closed loop frequency response and step-input closed loop time response were also obtained but not shown here due to space limitation. These measurements determined a closed loop bandwidth of 438 Hz, a peak overshoot of 68%, and a steady state error of $0 \mu\text{rad}$ as expected in a type I system. Good agreement was obtained between theory and experiment for all of the above measurements.

An optimization of the type I compensation was then carried out and has resulted in a predicted rms residual tracking accuracy of $1.1 \mu\text{rad}$, phase margin of 53 degrees, gain margin of 4 dB, and peak overshoot of 37%. This optimization was done assuming that a high gain margin is not required because a much reduced controller parameter variation is expected due to digital implementation. Depending on particular requirements of a given tracking control loop system, the characteristics of the compensation can be selected and optimized to obtain the best trade-off between stability and accuracy.

In conclusion, analysis and measurements were presented which show the feasibility of using low cost fine steering mirrors and moderate sampling rates for discrete-time tracking control loops for optical communications.

The author thanks C. C. Chen, E. H. Kopf, and J. R. Lesh for many valuable discussions. This work was carried out by the Jet Propulsion Laboratory, California Institute of Technology, under contract with the National Aeronautics and Space Administration.

References

1. C. C. Chen, H. Ansari, and J. R. Lesh, "Precision Beam Pointing for Laser Communication System using a CCD-Based Tracker," OE/Aerospace 93, Proc. Soc. Photo-Opt. Instrum. Eng. 1949-15, (April 1993).
2. "A Study to Define the Impact of Laser Communication Systems on their Host Spacecraft", Hughes Aircraft Co., Final Report NASA-CR-175272, (April 1984).
- 3) M. Wittig, L. Van Holtz, D.E.L. Tunbridge, H.C. Vermeulen, "In-Orbit Measurements of Microaccelerations of ESA's Communication Satellite OLYMPUS", Free-Space Laser Communication Technologies II, Proc. Soc. Photo-Opt. Instrum. Eng. 1218, (January 1990).
4. G. F. Franklin, J. D. Powell, and M. L. Workman, "Digital Control of Dynamic Systems," Second Edition, Addison-Wesley, (1990).

Figure captions

Figure 1 Block diagram of tracking control loop

Figure 2 Frequency response of fine steering mirror

Figure 3 Open-loop frequency response including compensation

Figure 4 Disturbance rejection of tracking control loop

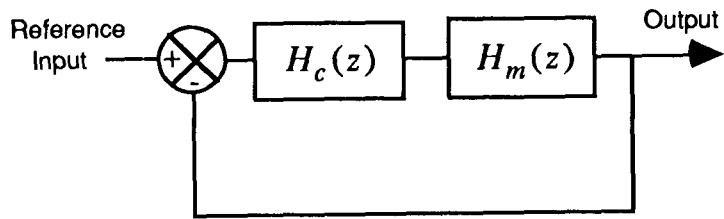


Figure 1 Block diagram of tracking control loop

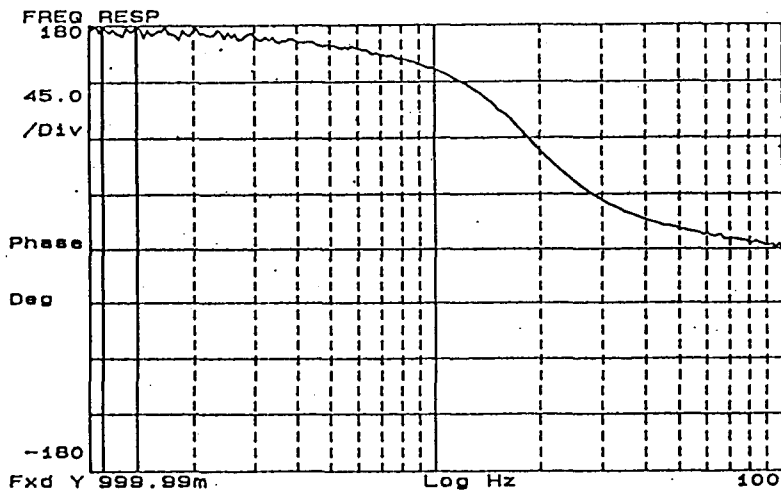
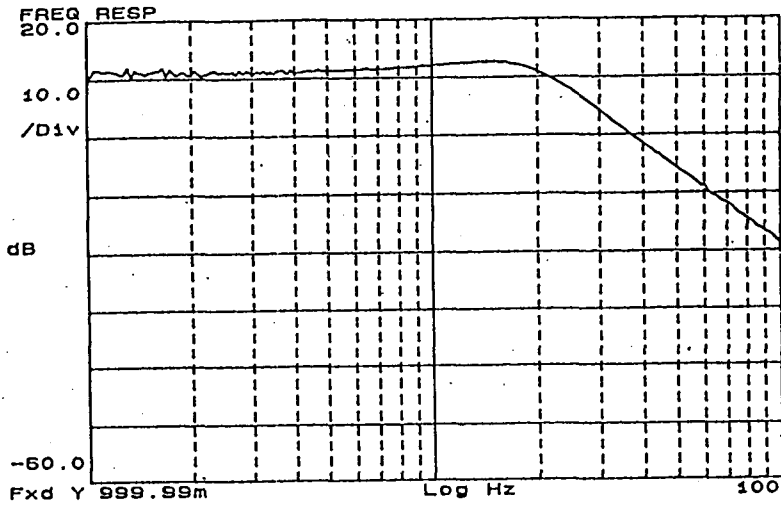


Figure 2 Frequency response of fine steering mirror

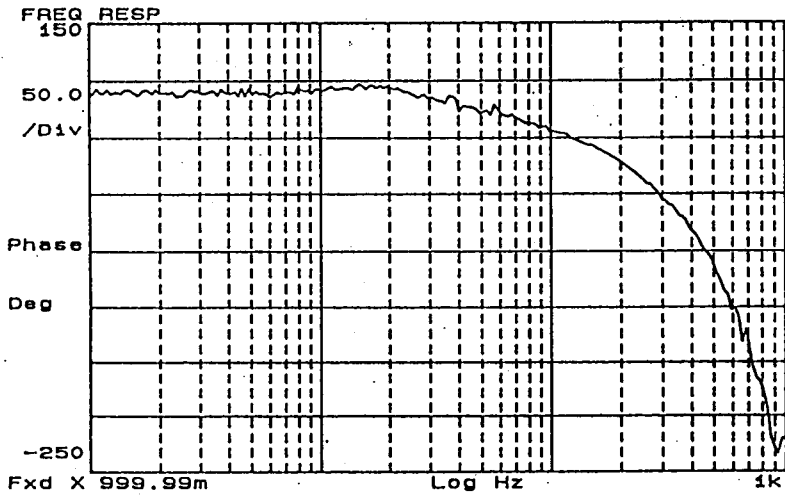
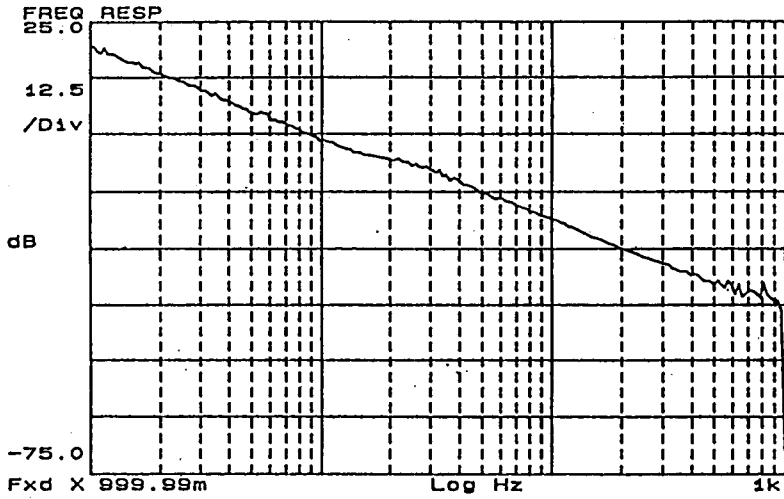


Figure 3 Open-loop frequency response including compensation

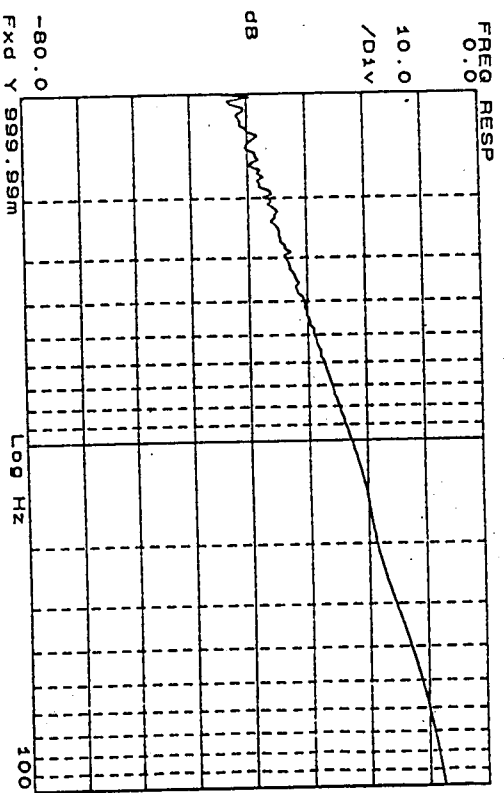


Figure 4 Disturbance rejection of tracking control loop